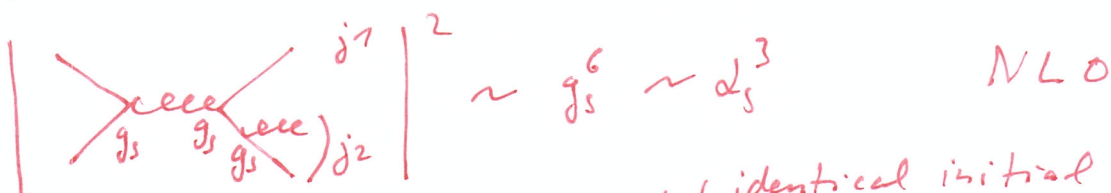


To Fig. 2.3

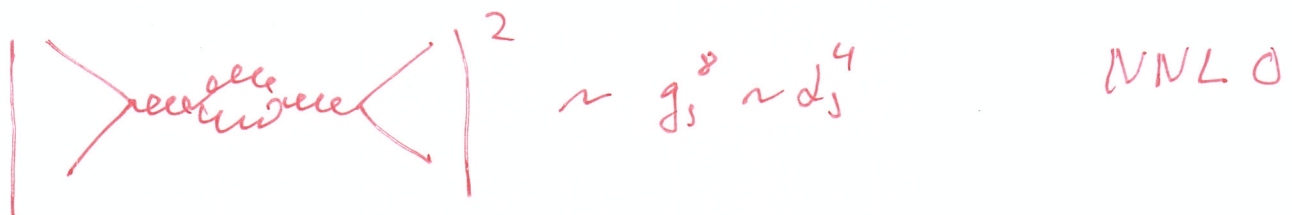
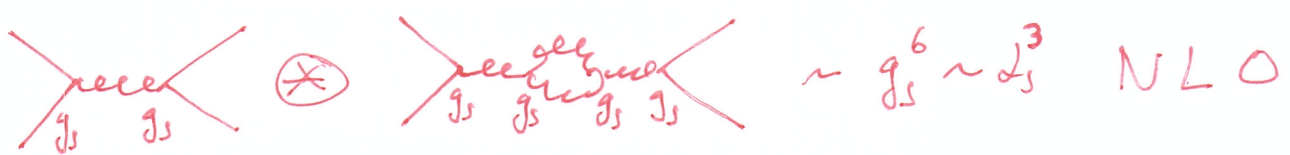
The bottom right diagram (loop) contributes to the NLO via interference!

The listed diagrams do not represent e.g. a scattering process:

~~PPF~~ parton + parton \rightarrow 2 + partons (e.g. $pp \rightarrow 2\text{jets} +$)
 $g_s^2 = 4\pi\alpha_s$



interference term! (identical initial & final state)



particle to the beam are calculated.

$$d_{ij} = \min(p_{Ti}^{2p}, p_{Tj}^{2p}) \frac{\Delta R_{ij}^2}{R^2}, \quad d_{iB} = p_{Ti}^{2p} \quad (2.18)$$

where $\Delta R_{ij}^2 = (\eta_i - \eta_j)^2 + (\phi_i - \phi_j)^2$

η_i η_j !

jet object

2. If $d_{ij} < d_{iB}$, then the particles i and j are merged into a new single particle k , summing four-momenta of two initial particles by recombination scheme and step 1 is repeated.
3. If $d_{iB} < d_{ij}$, particle i is declared as a final-state jet and the wave removed from the list.

This procedure continues until all particles get clustered into jets. The value of the parameter p defines the three different sequential algorithms having distinct properties. For $p = 1$, we have k_t algorithm [43, 44], $p = 0$ gives the Cambridge/Aachen (C/A) algorithm [45] whereas $p = -1$ defines the anti- k_T algorithm [46]. The k_t algorithm involves clustering of soft particles first resulting in an area that fluctuates considerably. This algorithm is susceptible to the underlying and pileup events. The C/A algorithm involves energy independent clusterings. Both k_t and C/A produce jets of irregular shapes. Instead of jet analysis, these are widely considered for studying the jet substructure. The anti- k_T algorithm tends to cluster hard particles first and produces more jets with circular regular shapes. It is less sensitive to underlying and pileup events. It is the most preferred algorithm for jet studies at the LHC. Figure 2.10 shows the clustering of same particles but using the different jet algorithms.

A jet algorithm must specify how to combine the momenta of different partons or particles going to be clustered into a jet. This is given by the recombination scheme. The most widely used recombination scheme is the E -scheme [40] which

the same place should not modify the number of jets formed in an event. This implies that the output of the jet algorithm should remain the same if the energy of a particle is distributed among two collinear particles. According to the collinear safety property, the two cases shown in Fig. 2.9 (bottom) should always produce a single jet. If an algorithm produces zero or two jets after collinear splitting, then it is not collinear safe. The jet algorithms can be classified mainly into two types :

Cone algorithms - In the iterative cone (IC) algorithm [40], the jet is defined as a cone with fixed radius R in $\eta\text{-}\phi$ space drawn around the highest energy seed. The relative distance (d) of all the particles is iteratively calculated and compared with R . If the calculated $d < R$, the considered particles are clustered together in a jet and the directions of the clustered particles give the direction of the jet. On the other side i.e. if $d > R$, the considered particles initiate two different jets. The algorithm iterates until the cone is stable which means that the direction of sum of momentum of all the particles is same as that of the center of cone. But IC algorithm is not IRC safe. There is another cone algorithm, Seedless Infrared-Safe cone (SIS-Cone) [41], which is an exact seedless i.e. does not rely on seed threshold and is IRC safe. This is a complex approach which tests the stability of all subsets of particles and has a complexity of $\mathcal{O}(N2^N)$ for N particles. But this algorithm is much slower and hence not preferred.

recombination

But it's the only cone
usable in pQCD!

Sequential algorithms - The sequential algorithms [42] cluster the particles by defining a distance between pairs of particles and recombine the pair of closest particles successively. This is collinear and infrared safe algorithm. It is possible for the jet cones to overlap such that one particle is contained in more than one jet but the sequential algorithm never assigns a particle to more than one jet. The sequential algorithm is based on transverse momentum p_T of the particles and follows the below procedure :

1. First the distance d_{ij} between two particles i and j and distance d_{iB} of the

in a proton-proton collision, undergoing fragmentation and hadronization processes and forming a conical jet with radius R. The jet structure was observed for the first time in hadron production of e^+e^- annihilation process at SLAC in 1975 [37]. The partons can not be measured directly by the experiments because they can not exist freely in nature. The information about the dynamics of the partons can be obtained indirectly from jets. The configurations of high-energy quarks and gluons at short distances are truly reflected in the energy and angular distributions of the jets. Hence the jets are important to study. To perform the clustering of particles, a certain set of rules are followed in the form of jet algorithms.

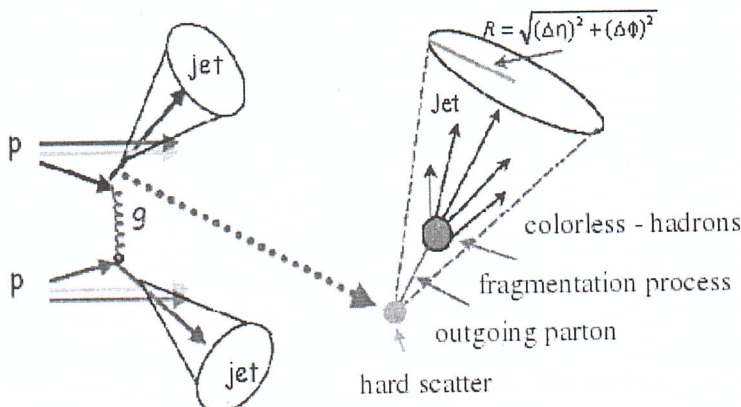


Figure 2.8: In a proton-proton collision, the outgoing partons of the hard scattering process undergo fragmentation and hadronization processes producing a shower of partons which get collimated into a conical jet with radius R.

2.4.1 Jet Algorithms

Jet algorithms [38] provide a set of rules which determine how the particles can be clustered into a jet. In a jet algorithm, usually one or more parameters are involved that indicate how close two particles must be for them to belong to the same jet. These parameters can either measure closeness in coordinate space (cone algorithms) or in momentum space (sequential algorithms). The jet algorithms are applicable on parton, particle and ~~calorimeter~~ levels. A recombination scheme is always associated with the detector.

fragmentation model. However, this model has problems in dealing with the decay of very massive clusters. — You don't discuss problems of the string model either ...

2.3.2 Underlying Event

Due to the composite nature of the protons, their collisions are not clean events.

The event structure is significantly more complex than that of the lepton collisions.

The final states of the collisions involve the multi-particle calculations. In a high energy proton-proton collisions, the underlying event (UE) includes the effects which are not coming from the primary hard scattering process. The UE includes the contributions from relatively small momentum transfer processes : initial and final-state radiations (ISR, FSR), leftover partons in the collisions called beam remnants and multiple parton interactions (MPI). Due to composite nature of proton, the remaining two partons which do not participate in a hard collision may also interact giving rise to multiple parton interactions. The UE induces an additional energy in an event which is not related to the main hard interaction. This acts as an unavoidable background which needs to be removed. Hence, it is very crucial to study and understand the UE. The UE activity increases with Q and the center-of-mass energy \sqrt{s} . Figure 2.7 shows the complex variety of processes taking place in a single proton-proton collision.

The bunch of hadrons, produced from hadronization of quarks and gluons, gets collimated in the form of "jets" with the direction towards the direction of the initial parton that originated them. The jets are the final structures observed experimentally in the detectors. These act as a bridge between the elementary quarks and gluons of QCD and the final hadrons produced in high energy collisions. Therefore, at large momentum transfer of the interacting partons, the jets and their observables are the best tools to test the predictions of perturbative QCD. Also, the jet production is sensitive to the strong coupling constant α_s . The precise knowledge of the jet production cross-section can help to extract the value of α_s .

If you define acronyms, you have to use them ...

Slang

✓ Yes.

ing partons, which are constituents of two colliding hadrons and taking part in hard scattering process, can also develop parton showers, commonly known as Initial-State Radiation (ISR). The initial partons produce showers till they collide to initiate the hard scattering process. The final outgoing partons produced from a hard scattering process can also undergo parton showering giving rise to Final-State Radiation (FSR). A parton shower terminates when the scale Q is below the hadronization scale ~ 1 GeV for QCD.

At the end of the shower, there is a decrease in the energy of partons due to successive emission of gluons. Due to this, the coupling constant of QCD α_s grows and QCD is not applicable any more. This leads to the confinement of colored quarks and gluons into the color-neutral composite particles called hadrons and this process is known as hadronization. The hadronization takes place at low momentum transfer and hence is non-perturbative in nature. Although no exact theory for hadronization is known, the different phenomenological models have been developed to simulate the hadronization process. The two main models implemented in Monte Carlo event generators to simulate the hadronization process are :

Lund String Model - In the Lund string model of hadronization [32], the highly energetic gluons are treated as field lines. Due to the gluon self-interaction, the gluons are attracted to each other forming a narrow tube or string of strong color field between a $q\bar{q}$ pair. This model is based on an observation that at distances greater than about a femtometre (fm)⁷, the potential energy $V(r)$ of colored quarks grows linearly with the increase in distance between them (r) as :

$$V(r) = \kappa r \quad (2.17)$$

where $\kappa \sim 1$ GeV/fm² is the tension of the string connecting the quarks. When the q and \bar{q} are pulled apart from each other move apart, the gluonic string stretches.

⁷ 1 femtometre = 1×10^{-15} metres

In a proton-proton collision, the cross-section of a hard scattering process can be written as :

$$\sigma_{P_1 P_2 \rightarrow X} = \sum_{i,j} \int dx_1 dx_2 f_{i,P_1}(x_1, \mu_f) f_{j,P_2}(x_2, \mu_f) \times \hat{\sigma}_{ij \rightarrow X} \left(x_1 p_1, x_2 p_2, \alpha(\mu_r^2), \frac{Q^2}{\mu_f^2} \right) \quad (2.16)$$

where f_i and f_j are the proton PDFs which depend on momentum fractions x_1 and x_2 of parent protons P_1 and P_2 respectively as well as on the factorization scale μ_f . The sum extends over all contributing initial-state parton flavours i, j . The cross-section for the production of final state X at parton level ($\hat{\sigma}_{ij}$) depends on the final state phase, the factorization scale μ_f and the renormalization scale μ_r . Figure. 2.5 illustrates the factorization into the PDFs and the hard scattering cross-section in a proton-proton collision.

The PDFs of the proton are a necessary input to almost all theory predictions of a proton-proton collision. The QCD does not predict the parton content of the proton. So the shapes of PDFs are determined in fits to experimental measurements of different experiments. The dependence of PDFs on μ_f is given by the Dokshitzer-Gribov-Lipatov-Altarelli-Parisi (DGLAP) [23–25] equations which use α_s and the RGE as inputs. The knowledge of proton PDFs mainly comes from the Deep-Inelastic Scattering (DIS) HERA, fixed-target and Tevatron data. The LHC data has a potential to improve constraints of the PDFs further as done in one of the recent CMS measurements [26]. There are several groups which determine the PDFs using various minimization methods, phenomenological approaches, and the strategies to estimate the uncertainties. The global PDFs are the CTEQ [27], MMHT [28], NNPDF [29], ABM [30] and HERAPDF [31] at LO, NLO and NNLO.

*not global
since only HERA data!*

scale of the Z boson mass $\alpha_s(M_Z)$. So, Eq. 2.13 can be expressed as :

$$\alpha_s(\mu_r, \alpha_s(M_Z)) = \frac{\alpha_s(M_Z)}{1 + \alpha_s(M_Z)b_0 \ln(\mu_r^2/M_z^2)} \quad (2.14)$$

Since α_s is ~~a~~ the free parameter of QCD theory, it ~~is always~~ extracted from ~~the~~ experimental measurements and evolved to the scale of the Z boson. According to Particle Data Group (PDG) [21], the current world average value of the strong coupling constant at the scale of mass of Z boson is $\alpha_s(M_Z) = 0.1181 \pm 0.0011$.

$$\alpha_s(M_Z) = 0.1181 \pm 0.0011 \quad (2.15)$$

This value is derived using data from deep inelastic scattering process, electron-positron annihilation processes, hadronic τ lepton decays, lattice QCD calculations and electroweak precision fits. The different experimental determinations of the strong coupling constant evolved at the scale Q are shown as a function of Q in Fig. 2.4 which describe the running of the α_s up to the 1 TeV scale.

2.3 Hadronic Collisions

At ~~a~~ large momentum transfer, the collision between two hadrons can be visualized as an interaction between their constituents - quarks and gluons. In this thesis, we are studying the proton-proton collisions taking place at the Large Hadron Collider (LHC). A proton is a complex composite particle consisting of three valence quarks (uud), gluons for the exchange of the strong force and the sea quarks. The sea quarks consist of quark-antiquark pairs coming into and out of existence rapidly and continuously due to gluon colour field splitting. In any collision, ~~one of the~~ ~~most important quantities~~ to evaluate is the cross-section (σ) of a certain process which gives the probability that the two hadrons interact and give rise to that

enter the calculations beyond LO either due to loop or vertex corrections. These are overcome by a procedure known as renormalization, described in next section. Apart from the UV divergences, the QCD also suffers from infrared and collinear divergences (IRC) due to the presence of massless gluons and neglected quark masses. These need to be handled in pQCD calculations. The observable to be studied must be IRC safe.

2.2.2 Renormalization and Running of the Strong Coupling

The renormalization is a mathematical procedure which allows the finite calculation of momenta integrals of virtual loop by removing UV divergences. It introduces a regulator for the infinities, the renormalization scale μ_r . At first, the divergences are regularized temporarily by introducing a cut-off to the loop momenta at μ_r scale. Then the free parameters of the Lagrangian, i.e. the coupling constant are redefined or renormalized to absorb the UV divergences. Due to this, both $\alpha_s(Q)$ and observable X become a function of μ_r . The exact dependence of $\alpha_s(\mu_r^2)$ on μ_r is described by the renormalization group equation (RGE) [18] which determines the running of $\alpha_s(\mu_r^2)$. According to RGE, the dependence of X on μ_r must cancel. Mathematically this can be expressed as :

$$\mu_r^2 \frac{d}{d\mu_r^2} X \left(\frac{Q^2}{\mu_r^2}, \alpha_s(\mu_r^2) \right) = \left(\mu_r^2 \frac{\partial}{\partial \mu_r^2} + \mu_r^2 \frac{\partial \alpha_s(\mu_r^2)}{\partial \mu_r^2} \frac{\partial}{\partial \alpha_s(\mu_r^2)} \right) X = 0 \quad (2.9)$$

Using beta function $\beta(\alpha_s) = \mu_r^2 \frac{\partial \alpha_s(\mu_r^2)}{\partial \mu_r^2}$, Eq. 2.9 can be re-written as

$$\left(\mu_r^2 \frac{\partial}{\partial \mu_r^2} + \beta(\alpha_s) \frac{\partial}{\partial \alpha_s(\mu_r^2)} \right) X = 0 \quad (2.10)$$

↙ Same for QED.

not constant and depends on the separation between the interacting particles. It increases with the increase in the distance or decrease in the energy scale Q . At large distances or low energies, the quarks can never be found as free particles but exit in color neutral bound states known as hadrons. Hadrons are of two types : baryons and mesons. According to the quark model [2] every (anti-)baryon is made up of three (anti-)quarks and every meson is made up of a quark-antiquark pair. When the colored partons within a hadron are pulled farther and farther apart, there is an increase in the strength of force between them. This results in creation of new quark-antiquark pairs making it impossible to liberate a free quark or gluon. This property of QCD is known as confinement according to which at low energy, the partons are forever bound into hadrons such as protons (uud), neutrons (udd) etc. Although the gluons are massless ~~but~~ the confinement leads to the finite range of the strong interactions. On the other hand, at small distances, the strength of coupling decreases. The quarks and gluons interact very weakly and behave as free particles. This property is known as asymptotic freedom. This indicates that perturbative theory is only applicable at high energies or small distances.

2.2.1 Perturbative Quantum Chromodynamics

At high energies, the property of asymptotic freedom allows a perturbative treatment in QCD calculations. In perturbative quantum chromodynamics (pQCD), any physical observable X such as cross-section of a scattering process, can be expanded as a perturbative series in terms of coupling constant α_s as :

$$X = \sum_{i=0}^N \alpha_s^n c_i = c_0 + \alpha_s^1 c_1 + \alpha_s^2 c_2 + \dots \quad (2.8)$$

where c_i are the perturbative coefficients. In a process, the pQCD calculation of X is determined by summing over the amplitudes of all Feynman diagrams contributing

of the gauge symmetry group $SU(3)_C$. The field tensor $F_{\mu\nu}^A$ is defined as

$$F_{\mu\nu}^A = \partial_\mu A_\nu^A - \partial_\nu A_\mu^A - g_s f_{ABC} A_\mu^B A_\nu^C$$

Summation implied
over identical indices
should be removed.

where g_s is the coupling constant determining the strength of the interaction between colored partons and f_{ABC} are the structure constants of the $SU(3)_C$ group. The last term in Eq. 2.3 is a non-abelian term which distinguishes QCD from QED and gives rise to a three- and a four-gluon vertex. In the term \mathcal{L}_{quarks} , $(D_\mu)_{ab}$ is the covariant derivative given by Eq. 2.4 and γ_μ are the Dirac γ -matrices.

$$(D_\mu)_{ab} = \partial_\mu \delta_{ab} + i g_s T_{ab}^A A_\mu^A \quad (2.4)$$

A_μ^A are the gluon fields with factors T_{ab}^A factors corresponding to the generators of the $SU(3)_C$ gauge group. The generators are represented via $T^A = \lambda^A/2$ by the Hermitian and traceless Gell-Mann matrices λ^A [16]. The generator matrices T^A follow the commutation relations :

$$[T^A, T^B] = i f_{ABC}^{\text{sum}} T^C \quad (2.5)$$

In \mathcal{L}_{QCD} , the classical contribution comes from \mathcal{L}_{gluons} and \mathcal{L}_{quarks} terms which give rise to the free quark- and gluon-field terms, and the quark-gluon interaction terms presented in Fig. 2.2. The cubic and quartic gluon self-interaction vertices proportional to g_s and g_s^2 , respectively, come into play due to the non-abelian property of QCD.

It is impossible to use perturbation theory on a gauge invariant Lagrangian without choosing a specific gauge in which to calculate. The usual gauge-fixing term

electromagnetic forces, respectively. $U(n)$ are the unitary and $SU(n)$ are the special unitary groups of degree n . The $SU(3)_C$ term defines the strong interaction between quarks and gluons mediated by gluons, with the three degrees of freedom of the color charge (C). The electromagnetic interaction of particles is explained by a well established modern theory called Quantum Electrodynamics (QED). In SM, the weak and electromagnetic interactions are combined by an electroweak symmetry theory, described by $SU(2)_L \otimes U(1)_Y$ gauge group. But this electroweak unification could not explain the occurrence of massive weak gauge bosons. This problem was solved by Brout-Englert-Higgs mechanism [10, 11]. The Higgs boson, named after Peter Higgs, is the field quantum of the Higgs field responsible for electroweak symmetry breaking. In SM, the Higgs field is a $SU(2)$ doublet which is a scalar under Lorentz transformations. The coupling of the bosons to the scalar Higgs field causes the spontaneous symmetry breaking which triggers the Higgs mechanism. After symmetry breaking, three of the four degrees of freedom in the Higgs field interact with the three weak gauge bosons (W^\pm and Z) and allows them to be massive, while the remaining one degree of freedom becomes the Higgs boson. Its existence was confirmed by the CMS [12] and ATLAS [13] collaborations in 2012, with the properties consistent with the SM. In contrast to the electroweak symmetry, the $SU(3)_C$ of the strong interaction is an exact symmetry and hence the gluons are massless. The strong interaction between quarks and gluons is described by theory called quantum chromodynamics (QCD), explained in detail in the next section.

2.2 Quantum Chromodynamics

The strong interactions between the quarks and gluons are described by a non-abelian gauge theory called quantum chromodynamics (QCD) [14, 15]. The gauge group of QCD is the special unitary group $SU(3)_C$ with color charges C as the generators of the gauge group. Color charge is the peculiar property of QCD and

fermions need not be elementary. Nuclei are either fermions or bosons for example.

mental particles and the three of the four known forces of interactions between them, as summarized in Fig. 2.1. According to the SM, the basic constituents of matter are the elementary particles i.e. without any internal structure, known as fermions and bosons. The fermions have half integral spin and obey Fermi-Dirac statistics. They follow the Pauli exclusion principle according to which two or more identical fermions cannot occupy the same quantum state. Each fermion has an associated anti-particle having the same properties but opposite-sign quantum numbers.

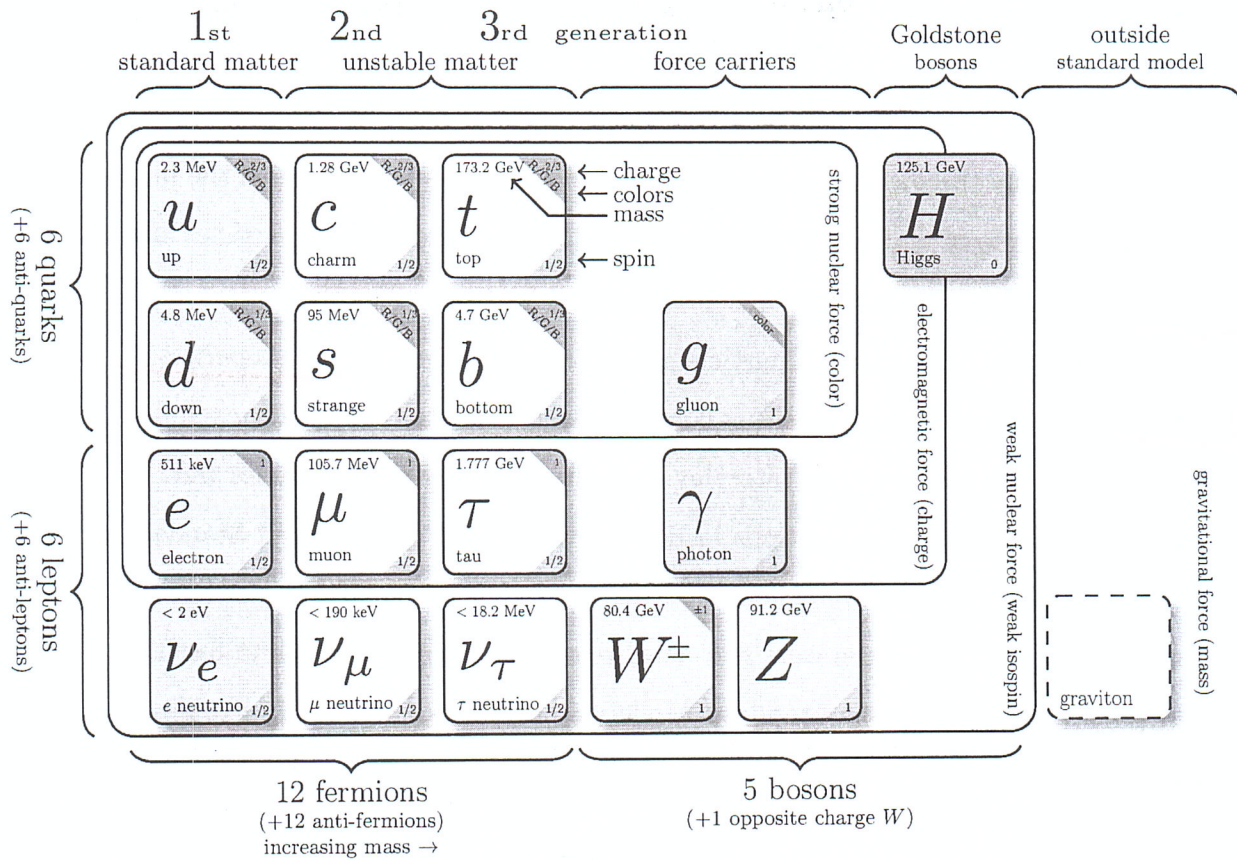


Figure 2.1: The Standard Model³ summarizing the properties of elementary particles known as fermions (leptons and quarks) grouped into three generations, gauge bosons as mediators for the interactions, the scalar Higgs boson and not incorporated graviton for the gravitational force.

³Source : <http://www.texample.net/tikz/examples/model-physics>

There are also 8 gluons...
if w^\pm are counted.

renormalization group equation (RGE)¹, which precisely describes the evolution of α_S at the renormalization scale of QCD.

The organization of this thesis² is as follows :

Chapter 2 gives a brief overview of the Standard Model of particle physics and the theory of strong interactions QCD, theory of hadron collisions as well as formation of jets and jet algorithms.

Chapter 3 deals with experimental apparatus which covers the details of the geometry of the CMS detector and its various sub-detectors.

Chapter 4 describes the methods of event generation used in different Monte-Carlo event generators, detector geometry simulation and reconstruction of the particles in the detector. This chapter also gives the details of the different approaches of jet reconstruction at CMS and applied jet-energy corrections along with the description of the software framework used in the analysis presented in the current thesis.

Chapter 5 presents the measurement of differential inclusive multijet event cross-sections and the cross-section ratio. The measurements are corrected for detector effects by unfolding procedure which is discussed in detail in this chapter. The sources of the experimental uncertainties are studied in detail.

Chapter 6 contains a detailed description of the NLO perturbative QCD theory predictions obtained using different PDF sets. The NLO predictions are corrected with the non-perturbative and electroweak corrections. The theoretical uncertainties are calculated from various sources. At the end of this chapter, the unfolded measurements are compared with the predictions at NLO in pQCD as well as with the predictions from several Monte Carlo event generators.

¹According to the RGE, the strong force becomes weaker at short distances corresponding to large momentum transfers. This is referred to a property of QCD called asymptotic freedom.

²The common unit convention based on International System of Units (SI) as followed in particle physics will be used throughout the thesis. In addition, the units electron volt (eV) and barn (b) are used for energy and interaction cross-section, respectively. The reduced Planck constant (\hbar) and speed of light (c) are set to unity, i.e. $\hbar = c = 1$.

These data sets are analyzed in detail to reveal the structure and characteristic properties of the fundamental particles.

To search for the very rare particles, to investigate the physics beyond SM, and to explore the regime of undiscovered physical laws, the particle accelerators have become bigger and complex over the past few decades. The Large Hadron Collider (LHC) is one of the biggest and the most powerful particle collider in which the protons are accelerated and collided at extremely high center-of-mass energies to probe their internal structure and the parton distribution functions (PDFs). The PDFs give the probability to find a parton at an energy scale Q carrying a fractional momentum x of the proton. Since the proton is not elementary and is made up of partons, the proton-proton (pp) collisions are viewed as interactions between their constituent partons. The final products of the scattering are observed by Compact Muon Solenoid (CMS), one of the four detectors of the LHC, located around the interaction points of the collisions. The scattering cross-section can be expressed as a sum in terms of increasing powers of the strong coupling constant α_S convoluted with PDFs. The lowest-order α_S^2 term represents the production of two partons in final states whereas terms of higher-order α_S^3 , α_S^4 etc. signify the existence of multi-partons in final states. The highly energetic final state partons emit quarks and gluons with lower energies and give rise to a parton shower (PS). The colored products of parton shower hadronize to a spray of colorless hadrons known as jets. The jets are the final structures observed in the detector. So they carry the significant information of the energy and direction of the initial partons and hence are important to study. The final partons also have the probability to radiate more gluons and quarks which also hadronize and result in multijets in the final state. At LHC, such events are produced in large number and are an important source for testing the predictions given by QCD. They also serve as an important background in the searches for new particles and physics beyond SM.

The inclusive multijet event cross-section σ_{i-jet} , given by the process